AIAA JOURNAL
Vol. 32, No. 2, February 1994

Thermomechanical Coupling Effects at High Flight Speeds

O. R. Odabas*
Ohio State University, Columbus, Ohio 43210
and
N. Sarigul-Klijn†
University of California, Davis, Davis, California 95616

A comparative numerical study of the coupled vs uncoupled thermal-structural analysis of viscoplastic structures is presented for supersonic and hypersonic flight speeds. In this study, deformations are assumed to be infinitesimal, and the viscoplastic behavior is described by using a unified constitutive model. The Galerkin finite element method is utilized along with a time-marching scheme to predict the quasistatic thermomechanical behavior of inelastic structures with rate and temperature-dependent material properties. In the coupled analysis, the displacements and temperature distribution at every time step are computed at once by solving the system of equations directly. The results indicate that the magnitude of coupling decreases with the increase in temperature and the decrease in internal dissipation.

I. Introduction

THE history of theoretical work on coupled thermomechanics of solids goes back to the mid-nineteenth century as described in Ref. 1. The early models incorporated the Newman-Duhamel equations in conjunction with linear elastic analysis to predict thermomechanical behavior. This one-way coupled (uncoupled) formulation was sufficient for the analysis of the Hookean materials. In linear thermoelasticity, for most of the engineering materials, only dilatational deformations cause temperature changes. These changes are small, and they vanish after a complete tension-compression cycle. The inertia terms are also comparatively small. Therefore, uncoupled quasistatic analysis of linear thermoelasticity problems introduces only a small error.[2,3]

For inelastic materials, however, processes resulting from inelastic deformations generate heat, raising the temperature irreversibly. Consequently, this increase in temperature changes the stresses. By the turn of the century, the mechanism of the two-way coupling between stress and temperature distributions was well understood. Experimental studies showed that the coupling between the deviatoric components of stress and temperature fields becomes significant for inelastic materials.[4,5] But there was a limited amount of work in this area until recently.

In the last couple of decades, increasing interest in design of high-speed flight vehicles brought attention to advanced analysis techniques and technologies. The hypersonic vehicles have to operate in severe aerothermal environments. Moreover, their aerodynamic characteristics as well as their structural integrity must be maintained in very strict tolerances. One of the major challenges is the evaluation of the structural response at high temperatures under steep temperature and stress gradients induced by pressure distribution, skin friction, and aerodynamic heating. Elevated temperatures degrade the load-carrying capabilities of materials. Besides this degradation, most metals demonstrate viscoplastic behavior when the temperature exceeds 40% of their melting temperatures.[6] The classical analysis techniques may not be sufficient under these conditions. In fact, the results of uncoupled analyses can be as much as 10% different from the results of coupled analyses.[7] Therefore, the analysis of thermomechanical coupling may be necessary, at least in the failure analysis stage, depending on the degree of material inelasticity and the deformation pattern.

On one hand, it was argued that, for a hypersonic vehicle, aerodynamic heating would be so large that thermal energy converted from mechanical energy would be negligible.[6] But this argument is not supported by experimental or computational evidence. On the other hand, it is known that the thermomechanical process becomes more rate sensitive at high temperatures, which, in turn, makes materials more susceptible to coupling. A number of researchers[8–10] attempted to predict the coupled inelastic material response; however, the number of comparative studies on the effects of coupling is very limited.[7,11] Furthermore, to the authors' knowledge, a thorough analysis showing the temperature applicability range of the uncoupled formulation is not available.

The study presented here addresses the issue of the magnitude of thermomechanical coupling that exists at different temperature levels. In the formulation, the inertia terms are assumed to be negligible and deformations are assumed to be infinitesimal. An extended Bodner-Partom constitutive model that also includes thermal effects is employed.[12] The spatial coordinates of the problem space are discretized by utilizing the standard Galerkin finite element approach. A finite difference method is employed for the discretization of the time domain. The uncoupled analysis is performed by solving the heat conduction equation separate from the equilibrium equations. The temperature changes are taken into account in the stress-strain equations. The coupled analysis is performed by solving the coupled heat conduction equation and the equilibrium equations at the same time. At every time step, the system equations are solved iteratively and the material properties are updated using the current temperature distribution. The paper begins with the formulation of coupled thermoviscoplasticity, followed by the description of the constitutive model. Next, a three-dimensional finite element formulation is presented. Finally, the magnitude of thermomechanical coupling is evaluated for a superalloy, B1900 + Hf, which is the only material for which elevated temperature data were available.

II. Theoretical Formulation

A viscoplastic solid domain with interior V and boundary ∂V is assumed to be undergoing infinitesimal deformations quasistatically. The formulation for this boundary-value problem involves the conservation equations of continuum thermomechanics, the second law of thermodynamics, and the constitutive assumptions. The mass and angular momentum conservation are achieved by imposing material incompressibility and the symmetry of the

Presented as Paper 92-5018 at the AIAA 4th International Aerospace Planes Conference, Orlando, FL, Dec. 1–4, 1992; received Dec. 30, 1992; revision received July 6, 1993; accepted for publication July 6, 1993.

*Graduate Research Associate, Department of Aeronautical and Astronautical Engineering. Student Member AIAA.

†Associate Professor of Aeronautical Science and Engineering, Department of Mechanical, Aeronautical, and Materials Engineering. Member AIAA.

Table 1 Temperature-independent material constants for B1900 + Hf[15]

m_1, MPa	0.27
m_2, MPa	1.52
Z_1, MPa	3,000
Z_3, MPa	1,150
r_1	2
r_2	2
D_0, 1/s	10,000

stress tensor. Utilizing the internal state variable formulation discussed by Allen,[1] the governing equations are stated as follows.

A. Governing Equations

In accordance with the assumptions, the strain-displacement equations are linearized and the acceleration terms in the equilibrium equations are neglected.

The rate form of the equilibrium equations, which is used to solve for, is written as

$$\frac{\partial \dot{\sigma}_{ki}}{\partial x_k} + \dot{b}_i = 0 \tag{1}$$

where σ_{ki} are the stress components, b_i are the components of body force per unit mass, and a dot is the differentiation with respect to time. The energy equation is

$$\rho \dot{e} = \sigma_{ik}\dot{\varepsilon}_{ik} - \frac{\partial q_i}{\partial x_i} + \rho \dot{r} \tag{2}$$

where ρ is the mass density, e is the internal energy per unit mass, ε_{ik} are the total strain components, q_i is the heat flux, and r is the internal heat sink/source per unit volume.

The rate form of the strain-displacement equations can be linearized by neglecting the second-order terms in the Green strain tensor as

$$\dot{\varepsilon}_{ij} = \frac{1}{2}\left(\frac{\partial \dot{u}_j}{\partial x_i} + \frac{\partial \dot{u}_i}{\partial x_j}\right) \tag{3}$$

where u_i are the displacement components.

The rate form of the stress-strain equations

$$\dot{\sigma}_{ij} = C_{ijkl}(\dot{\varepsilon}_{kl} - \gamma_{kl}\dot{T}) = C_{ijkl}(\dot{\varepsilon}_{kl} - \dot{\varepsilon}^p_{kl} - \gamma_{kl}\dot{T}) \tag{4}$$

where C_{ijkl} are the material constants, $\dot{\varepsilon}^p_{kl}$ are the plastic strain components, γ_{kl} are the thermal expansion coefficients, and T is the temperature.

Inelastic processes are irreversible in nature, and entropy production inequality must be imposed on the previous equations. For any process

$$T\,\mathrm{d}s \geq \mathrm{d}Q \qquad S = \rho s \tag{5}$$

where ρ is the entropy per unit volume, and Q is the heat energy.

B. Second Law of Thermodynamics

The entropy production inequality can also be written in the following form:

$$T\rho\dot{s} \geq -q_{i,i} + \rho\dot{r} \tag{6}$$

To impose the inequality, the Helmholtz free energy h may be employed as

$$h = e - Ts \tag{7}$$

By differentiating e in time, replacing the term $\rho T\dot{s}$ with $\rho\dot{e} - \rho s\dot{T} - \rho\dot{h}$ in the inequality, and using energy equation (2), one can obtain constraints. The inequality introduces the following constraints[1] that hold for all processes:

$$h = h(\varepsilon_{ij}, T, \alpha^v_{ij}) \tag{8}$$

$$\sigma_{kl} = \sigma_{kl}(\varepsilon_{ij}, T, \alpha^v_{ij}) = \rho\frac{\partial h}{\partial \varepsilon_{kl}} \tag{9}$$

$$s = s(\varepsilon_{ij}, T, \alpha^v_{ij}) = \frac{\partial h}{\partial T} \tag{10}$$

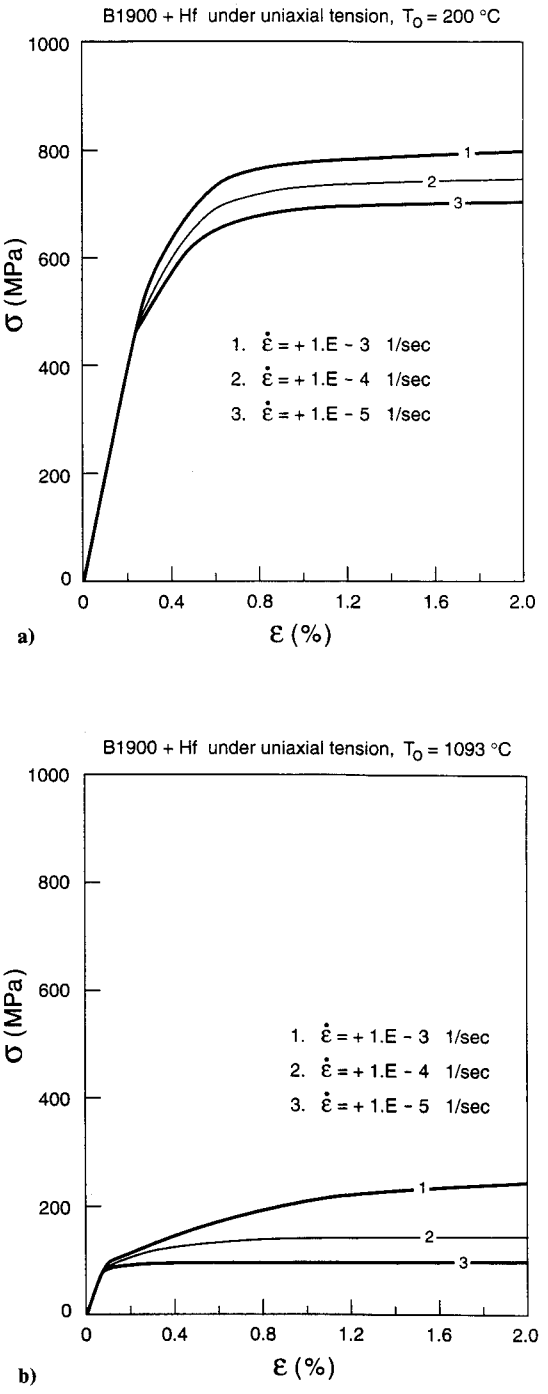

Fig. 1 Response of the structure to different strain rates at temperatures of a) 200°C and b) 1093°C.

The entropy production inequality becomes evident as internal and heat conduction dissipation ≥ 0.

Here α_{ij}, $\nu = 1, \ldots, n$, are the internal state variables that are detailed in the next section. The Helmholtz free energy represents the recoverable energy in any process. Based on experimental observation, Allen[1] suggested that elastic strains were the sole source of free energy in viscoplastic materials during isothermal processes. Following this suggestion, the coupled heat conduction equation for an isothermal process can be written as follows:

$$-\rho T\frac{\partial^2 h}{\partial \varepsilon_{ij}\partial T}\dot{\varepsilon}_{ij} + \rho T\frac{\partial^2 h}{\partial T^2}\dot{T} + \rho T\frac{\partial^2 h}{\partial \alpha^{\nu}_{ij}\partial T}\dot{\alpha}^{\nu}_{ij} + \rho\frac{\partial h}{\partial \alpha^{\nu}_{ij}}\dot{\alpha}^{\nu}_{ij} = -q_{i,i} + \rho\dot{r} \tag{11}$$

If the internal state variable evolution laws $\dot{\alpha}^{\nu}_{ij}$, $\nu = 1, \ldots, n$, and the Helmholtz free energy function h in Eq. (8) are given, the problem is completely defined.

C. Constitutive Model

The Bodner-Partom constitutive model is a unified model. It is independent of a yield criterion. The total strain rate is considered to be separable into elastic, inelastic, and thermal components that are functions of state variables at all stages of loading and unloading conditions. The model has been under development for more than two decades. The current version of the model can predict isotropic and directional hardening and also includes temperature effects.

Flow Law

For the inelastic strain rate component, the isotropic form of the Prandtl-Reuss law is assumed:

$$\dot{\varepsilon}^{p}_{ij} = \lambda S_{ij} \tag{12}$$

$$\dot{\varepsilon}^{p}_{kk} = 0 \tag{13}$$

where $\lambda > 0$ and S_{ij} are the deviatoric stress components given by

$$S_{ij} = \sigma_{ij} - \frac{1}{3}\delta_{ij}\sigma_{kk} \tag{14}$$

and $\dot{e}^{p}_{kk} = 0$ denotes the plastic incompressibility condition.

Kinematic Equations

Squaring Eq. (12) leads to

$$\lambda^2 = \frac{D_2^p}{J_2} \tag{15}$$

where D_2^p and J_2 are the second invariants of the strain rate and stress tensors, respectively,

$$J_2 = \tfrac{1}{2}S_{ij}S_{ji} \tag{16}$$

$$D_2^p = \tfrac{1}{2}\dot{\varepsilon}^{p}_{ij}\dot{\varepsilon}^{p}_{ji} \tag{17}$$

Experimental observations have shown that the uniaxial plastic strain rate is a function of stress.[12] Bodner and Partom generalized this statement for the multidimensional case:

$$D_2^p = D_0^2 \exp\left[-\left(\frac{Z^2}{3J_2}\right)^n\right] \tag{18}$$

where D_0 is the limiting strain rate in shear, n is a temperature-dependent material parameter, and Z is a load-history-dependent parameter, known as internal state variable. Using Eqs. (12–15) and Eq. (18), one can obtain plastic strain rates as

$$\dot{\varepsilon}^{p}_{ij} = \frac{S_{ij}}{\sqrt{J_2}} D_0 \exp\left[-\frac{1}{2}\left(\frac{Z^2}{3J_2}\right)^n\right] \tag{19}$$

Evolution Equations of the Internal State Variable

The internal state variable Z consists of isotropic Z^I and directional Z^D components,

$$Z = Z^I + Z^D \tag{20}$$

The evolution equation proposed for the isotropic hardening component[12] is

$$Z^I(t) = m_1\left[Z_1 - Z^I(t)\right]\dot{W}_p(t) - A_1 Z_1\left[\frac{Z^I(t) - Z_2}{Z_1}\right]^{r_1} \tag{21}$$

where m_1 is the hardening rate, Z_1 is the limiting (saturation) value of Z^I, Z_2 is the minimum value of Z^I at a given temperature, $\dot{W}_p = \sigma_{ij}\dot{\varepsilon}^{p}_{ij}$ is the plastic work rate, A_1 and r_1 are temperature-dependent material constants, and $Z^I(0) = Z_0$.

The evolution form of the directional hardening component[12] is defined as

$$Z^D(t) = \beta_{ij}(t)\,\theta_{ij}(t) \tag{22}$$

where θ_{ij} are the direction cosines of the current stress state,

$$\theta_{ij}(t) = \frac{\sigma_{ij}(t)}{\left[\sigma_{kl}(t)\,\sigma_{kl}(t)\right]^{1/2}} \tag{23}$$

The evolution equation for β_{ij} has the same general form as that for isotropic hardening but has tensorial character:

Table 2 Temperature-dependent material constants for B1900 + Hf[15]

T, °C	0	200	400	538	760	871	982	1093
E, GPa	198.7	198	189.6	179.58	156.75	142.42	126.29	108.44
G, GPa	80.65	77.78	75.11	72.51	65.49	60.06	52.96	43.93
γ, 10^{-5}l/°C	1.15	1.34	1.36	1.39	1.51	1.56	1.59	1.63
k, N/°Ks	4.1327	5.3316	6.5363	7.3675	9.023	9.8683	10.7135	11.5588
ρc_p, MPa/K	1.364	1.516	1.669	1.775	1.993	2.105	2.217	2.329
n	1.055	1.055	1.055	1.055	1.055	1.03	0.085	0.07
Z_0, MPa	2700	2700	2700	2700	2700	2400	1900	1200
Z_2, MPa	2700	2700	2700	2700	2700	2400	1900	1200
A_1, l/s	0	0	0	0	0	0.0055	0.02	0.25
A_2, l/s	0	0	0	0	0	0.0055	0.02	0.25

$$\dot{\beta}_{ij}(t) = m_2 [Z_3 u_{ij}(t) - \beta_{ij}(t)] \dot{W}_p(t)$$

$$-A_2 Z_1 \left[\frac{\beta_k l(t)\, \beta_k l(t)^{1/2}}{Z_1}\right]^{r_2} \xi_{ij}(t) \tag{24}$$

where

$$\xi_{ij}(t) = \frac{\beta_{ij}(t)}{\beta_{kl}(t)\, \beta_{kl}(t)^{1/2}} \tag{25}$$

where m_2 is the hardening rate; A_2, r_2, and Z_3 are temperature-dependent material constants; and $\beta_{ij}(0) = 0$.

III. Finite Element Formulation

For both uncoupled and coupled analyses, the unknowns of the problem are the displacements and the temperature values. The displacement rates $\dot{u} = \dot{u}(\dot{u}_1, \dot{u}_2, \dot{u}_3)$ within an element are approximated by

$$[\dot{u}] = [N]\,[\dot{d}] \tag{26}$$

and temperature rates are approximated by

$$[\dot{T}] = [\bar{N}]\,[\dot{\bar{T}}] \tag{27}$$

where $[N]$ is the matrix of shape functions for displacements, $[\bar{N}]$ is the vector of shape functions for temperature, $[\dot{d}]$ is the unknown vector of rate of nodal displacements, and $[\dot{\bar{T}}]$ is the unknown vector of rate of nodal temperatures.

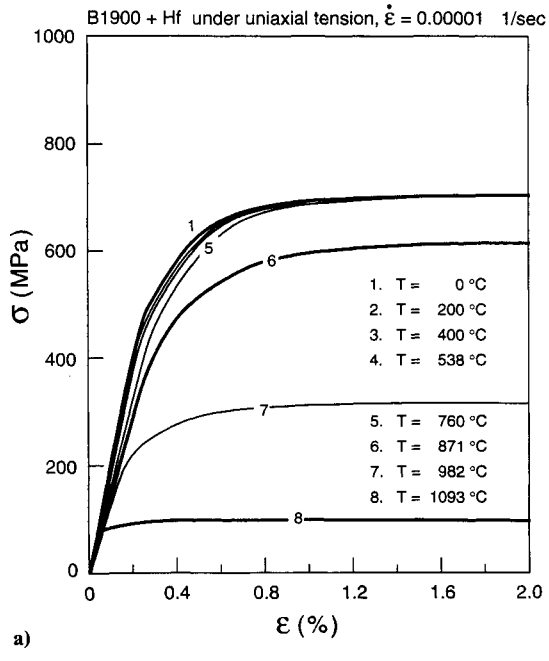

Fig. 2 Response of the structure to different temperatures at strain rates of a) 0.00001 1/s and b) 0.001 1/s.

A. Equilibrium Equations

The strain rates at the element level can be computed through strain-displacement rate equations:

$$[\dot{\varepsilon}] = [B]\,[\dot{d}] \tag{28}$$

where $[B]$ is the strain-displacement matrix. The discretized form of the equilibrium equations in rate form at element level becomes

$$\int_{V_e} [B]^T [C]\,[B]\, dV_e \{d\} - \int_{V_e} [B]^T [C]\,\{\gamma\}\,[N]\, dV_e \{\dot{\bar{T}}\}$$

$$= \int_{V_e} [B]^T [C]\,\{\{\varepsilon^p\} + [N]^T [b]\} + dV_e$$

$$+ \int_{\partial V_e} [N]^T [f]\, d\partial V_e \tag{29}$$

where f defines the surface tractions, $[C]$ is the material constants matrix, and V_e is the volume of the element. In the uncoupled analysis, the first integral is identified as $[M_{DD}]$ matrix, the temperature distribution is given, and the force vector consists of the rest of the terms as $[\dot{F}_D]$. In the coupled analysis, the first two integrals are named as $[M_{DD}]$ and $[M_{DT}]$ matrices, and the force vector consists of the terms on the right side as $[\dot{F}_D]$.

B. Coupled Heat Conduction Equation

If the Helmholtz free-energy function (8) is a function of elastic deformations and has the following form,[1]

$$h = h(\varepsilon_{kl}, T, \varepsilon^p_{kl}) \tag{30}$$

then the coupled heat conduction Eq. (2) becomes

$$-\sigma_{ij}\dot{\varepsilon}^p_{ij} + C_{ijkl}\gamma_{kl} T(\dot{\varepsilon}_{ij} - \dot{\varepsilon}^p_{ij}) + \rho c_v \dot{T} - (k_{ij} T_j)_{,i} - \rho r = 0 \tag{31}$$

where c_v is the specific heat at constant volume, and k_{ij} is the thermal conductivity tensor. Here the plastic work term is taken into account in full magnitude, but experimental evidence[13] demonstrates that a small portion of this energy goes to microstructural changes. Therefore, it is more appropriate to multiply the plastic work term with a dissipation factor η. For some typical engineering materials, the dissipation factor is between 0.8 and 0.9 at room temperature and reaches 1.0 at melting temperatures. Again, by employing Galerkin's approach and integrating the equation over the volume, the energy equation at the element level becomes

$$\int_{V_e} T [N]^T [C]\{\gamma\}[B][N]\, dV_e \{\dot{d}\} + \int_{V_e} \rho c_v [N]^T [N]\, dV_e \{\dot{\bar{T}}\}$$

$$+ \int_{V_e} \{[\nabla N]^T [k][\nabla N] - [N]^T [C]\{\gamma\}[\dot{\varepsilon}^p][N]\}\, dV_e \{\bar{T}\}$$

$$= \int_{V_e} [N]^T \{\eta[\sigma][\dot{\varepsilon}^p] + \rho \dot{r}\}\, dV_e + \int_{\partial V_e} [\bar{N}]^T q\, d\partial V_e \tag{32}$$

It may be noted that if the mechanical work terms are neglected in Eq. (32), the remaining equation is the discretized form of the classical time-dependent heat conduction problem. In this case, the second and the third integrals represent the $[M_{TT}]$ and $[K_{TT}]$ matrices, respectively, and the integrals on the right are the force vector $[\dot{F}_T]$. In the coupled analysis, the first two integrals are $[M_{TD}]$ and $[M_{TT}]$, the third integral is named as the $[K_{TT}]$ matrix, and the rest of the terms constitute the force vector $[\dot{F}_T]$. A short form of Eqs. (29) and (32) is given in next section.

IV. Solution Method

The uncoupled solution involves a standard heat transfer analysis followed by a viscoplastic structural analysis.[14] The parameters are updated using current temperature and displacement values at every time step. An algorithm for the coupled solution is presented next. It differs from the uncoupled solution in two ways. The heat transfer equation contains mechanical work terms, and the unknowns are computed at every time step. Viscoplastic constitutive models are, in general, stiff equations; therefore, special care must be given to step sizes. The first step in the solution process is finding the temperature distribution and the displacements and stresses for the initial conditions. Once the initial values are specified and the size of the time increment Δt is decided, marching in time may begin.

1) At $t = 0$, initialize T, σ_{ij}, and Z and material constants for each element.

2) Compute the plastic strain rate for each element from Eq. (19).

3). Assemble and solve discretized equilibrium and coupled heat conduction equations together at once; for all unknowns Eqs. (29) and (32) become

$$\begin{bmatrix} [M_{DD}] & [M_{DT}] \\ [M_{TD}] & [M_{TT}] \end{bmatrix} \begin{Bmatrix} \dot{d} \\ \dot{\bar{T}} \end{Bmatrix} + \begin{bmatrix} [0] & [0] \\ [0] & [K_{TT}] \end{bmatrix} \begin{Bmatrix} d \\ \bar{T} \end{Bmatrix} = \begin{Bmatrix} \dot{F}_D \\ \dot{F}_T \end{Bmatrix}$$

4) Compute strain rates for each element from Eq. (28).

5) Compute stress rates for each element from Eq. (4).

6) Compute $\dot{Z}$ for each element from the rate form of Eq. (20).

7) Integrate $\dot{\bar{T}}$, $\dot{d}$, $\dot{\sigma}_{ij}$, and $\dot{Z}$ and find current values.

8) Check if $t + \Delta_t < t_{\text{final}}$, adjust time step, and go to 2; otherwise stop.

Depending on the material type and strain rates, material constants may be updated at desired intervals. In the case of large thermal gradients, nodal values of material constants may be interpolated within each element for improved accuracy.

V. Numerical Examples

To demonstrate thermomechanical coupling in viscoplastic solids, a three-dimensional model of a simple rod made of a high-temperature superalloy (B1900 + Hf) is studied. Material constants of the Bodner-Partom constitutive model for B1900 + Hf are obtained from Ref. 15. Table 1 gives temperature-independent material constants for this material. Constitutive model temperature-dependent material coefficients along with Young's modulus, shear modulus, thermal expansion, heat conduction, and specific heat coefficients are given for a wide range of temperatures in Table 2.

At time zero, the rod with isotropic and homogeneous material properties is assumed to have a uniform temperature distribution and no stresses. To investigate the maximum possible temperature change due to coupling, the rod is thermally insulated on all boundaries, and there is no internal heat generation or loss. The rod is constrained on one end in the same direction as the applied force and is free to move in other directions. This way, boundary effects on the stress and displacement fields are eliminated. Also, there is no body force on the structure. Two different loading conditions are studied: uniaxial tension and uniaxial compression with time steps of 0.01 s.

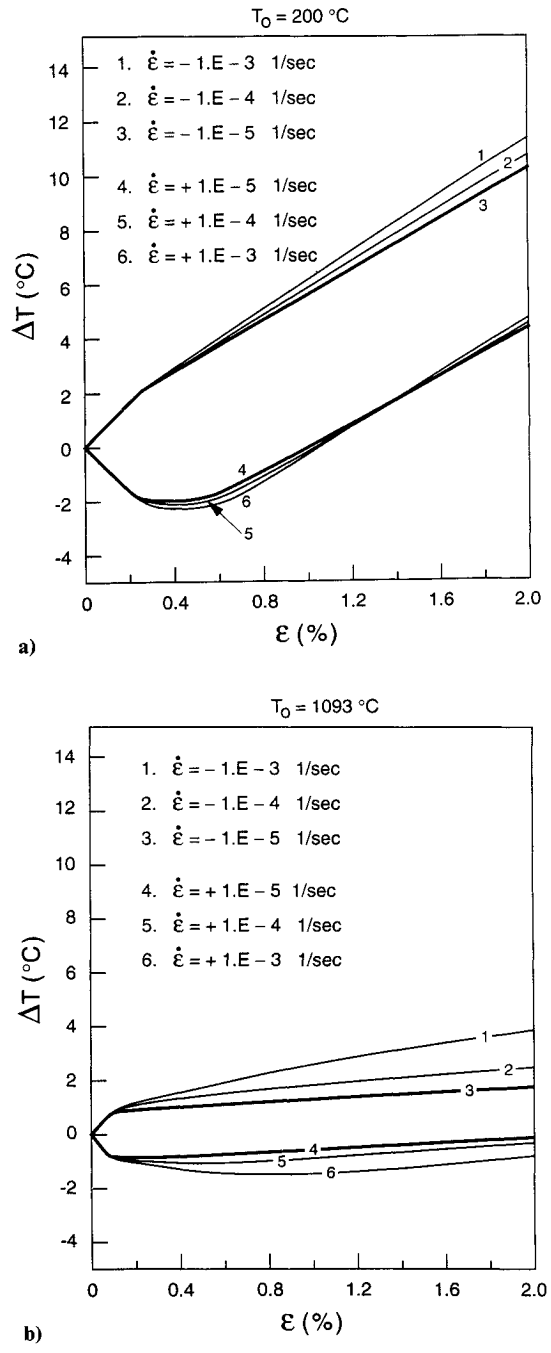

Fig. 3 Coupled analysis: temperature increase ΔT under different strain rates at temperatures of a) 200°C, uniaxial tension, and b) 1093°C, uniaxial compression.

A thermoviscoplastic structural analysis is performed for a wide range of temperatures between 0 and 1093°C and three strain rates. The maximum deformation limit is set to 2% at each case. The uncoupled analysis is achieved through the solution of equilibrium equations at every time step. In Fig. 1, the response of the structure is given for 200 and 1093°C. In Fig. 2, the responses to two different strain rates at increasing temperatures are plotted. Some significant features of the Bodner-Partom model can be observed in these results. Kinematic hardening, strain rate dependency, and temperature dependency are predicted by the constitutive equations. Above 760°C, the strength of the material decreases sharply, and it becomes more rate sensitive; see Fig. 2.

The results of coupled analysis are presented in Figs. 3 and 4. To capture the heating/cooling effect of elastic deformations, the rod is analyzed under uniaxial tension and compression. In tension, initial cooling due to expansion is followed by heating due to

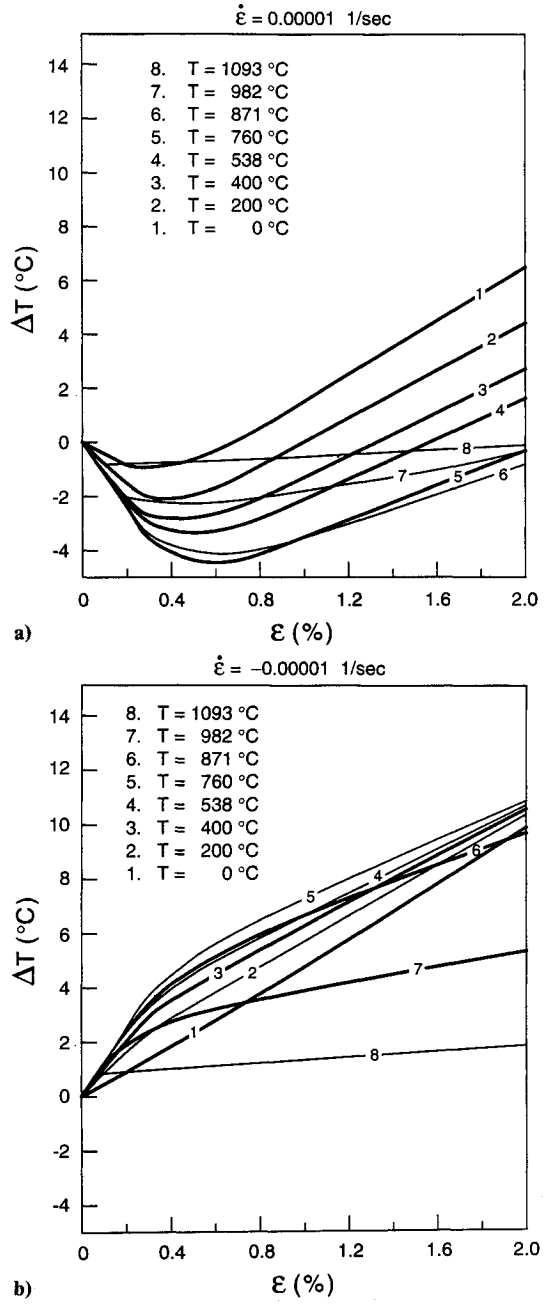

Fig. 4 Coupled analysis: temperature increase ΔT to different temperature conditions at strain rates of a) 0.00001 1/s, uniaxial tension, and b) 0.00001 1/s, uniaxial compression.

plastic work; see Fig. 3a. In compression, on the other hand, initial elastic deformations are compressive in nature, and they increase in temperatures; see Fig. 3b. The effect of strain rates on the coupling is shown for two temperatures. Increasing strain rates cause larger stresses that, in turn, generate more heat. In Fig. 4a uniaxial tension and in Fig. 4b compression with a strain rate of 0.0001 are plotted for different temperatures. Plastic work is the dominant term at low temperatures. But high temperatures degrade the material's strength; consequently, the material requires less plastic work for the same amount of strain. In addition, the heating/cooling effects of elastic deformations are increased due to high temperatures. Combining these two terms gives the overall magnitude of thermomechanical coupling, and its magnitude decreases with increasing temperatures. The temperature change resulting from mechanical processes is more significant at lower temperatures than at higher ones.

VI. Concluding Remarks

This paper is a study of thermomechanical coupling effects at temperature ranges of representative supersonic and hypersonic flight speeds. Because of the lack of experimental material data, this study has been limited to one superalloy. Two different analyses approaches were detailed; namely, uncoupled and coupled. The following conclusions are a result of numerical studies performed under small strain assumptions. For temperature values of up to 760°C coupled formulations must be used. It may be noted that this temperature level coincides with the temperatures encountered at supersonic speeds. Since the coupling effects are not strong beyond 760°C, it may be concluded that at hypersonic speeds uncoupled formulation is adequate.

References

[1]Allen, D. H., "Thermomechanical Coupling in Inelastic Solids," *Applied Mechanics Reviews*, Vol. 44, No. 8, 1991, pp. 361–373.

[2]Boley, B. A., and Weiner, J. H., *Theory of Thermal Stresses*, Wiley, New York, 1960, Chaps. 2–4.

[3]Nowinski, J. L., *Theory of Thermoelasticity with Applications*, Sijhoff & Nordhoff, Alphen aan den Rijn, The Netherlands, 1978, Chaps. 3, 5.

[4]Dillon, O. W., Jr., "An Experimental Study of the Heat Generated During Torsional Oscillations," *Journal of Mechanics and Physics of Solids*, Vol. 10, July-Sept. 1962, pp. 235–244.

[5]Farren, W. S., and Taylor, G. I., "The Heat Developed During Plastic Extension of Metals," *Proceedings of the Royal Society of London*, Vol. 107, March 1925, pp. 422.

[6]Thornton, E. A., "Thermal Structures: Four Decades of Progress," *Proceedings of the AIAA/ASME/ASCE/AHS/ASC 31st Structures, Structural Dynamics, and Materials Conference*, AIAA, Washington, DC, 1990, pp. 794–814, (AIAA Paper 90-0971).

[7]Banas, A., Hsu, T. R., and Sun, N. S., "Coupled Thermoelastic-Plastic Stress Analysis of Solids by Finite-Element Method," *Journal of Thermal Stresses*, Vol. 10, Oct.-Dec. 1987, pp. 319–344.

[8]Allen, D. H., "A Prediction of Heat Generation in a Thermoviscoplastic Uniaxial Bar," *International Journal of Solids and Structures*, Vol. 21, No. 4, 1985, pp. 325–342.

[9]Cernocky, E. P., and Krempl, E., "A Theory of Thermoviscoplasticity Based on Infinitesimal Total Strain," *International Journal of Solids and Structures*, Aug. 1980, pp. 723–741.

[10]Ghoneim, H., and Matsouka, S., "Thermoviscoplasticity by Finite Element: Tensile and Compression Test," *International Journal of Solids and Structures*, Vol. 23, No. 8, 1987, pp. 1133–1143.

[11]Argyris, J. H., Vaz, L. E., and William, K. J., "Integrated Finite-Element Analysis of Coupled Thermoviscoplastic Problems," *Journal of Thermal Stresses*, Vol. 4, April-June 1981, pp. 121–153.

[12]Miller, A. K. (ed.), *Unified Constitutive Equations for Creep and Plasticity*, Elsevier Applied Science Publishers, New York, 1987, pp. 273–301.

[13]Taylor, G. I., and Quinney, H., "The Latent Energy Remaining in a Metal After Cold Working," *Proceedings of the Royal Society of London*, Vol. 143, Jan. 1934, pp. 307–326.

[14]Thornton, E. A., Oden, J., Tworzydlo, W. W., and Youn, S. K., "Thermoviscoplastic Analysis of Hypersonic Structures Subjected to Severe Aerodynamic Heating," *Journal of Aircraft*, Vol. 27, No. 9, 1990, pp. 826–835.

[15]Chan, K. S., Lindholm, U. S., and Bodner, S. R., "Constitutive Modeling for Isotropic Materials (HOST)," Southwest Research Inst., Final Rept., San Antonio, TX, NASA CR-182132, June 1988.